N91-16685

AIR-GROUND INTERFACE: SURFACE WAVES, SURFACE IMPEDANCE AND ACOUSTIC-TO-SEISMIC COUPLING COEFFICIENT

Gilles Daigle and Tony Embleton
Division of Physics
National Research Council
Ottawa CANADA K1A 0R6

ABSTRACT

In atmospheric acoustics, the subject of surface waves has been an area of discussion for many years. The existence of an acoustic surface wave is now well established theoretically. The mathematical solution for spherical wave propagation above an impedance boundary includes the possibility of a contribution that possesses all the standard properties for a surface wave. Surface waves exist when the surface is sufficiently porous, relative to its acoustical resistance, that it can influence the airborne particle velocity near the surface and reduce the phase velocity of sound waves in air at the surface. This traps some of the sound energy in the air to remain near the surface as it propagates. Above porous grounds, the existence of surface waves has eluded direct experimental confirmation (pulse experiments have failed to show a separate arrival expected from the reduced phase speed) and indirect evidence for its existence has appeared contradictory. In PART I of this paper the experimental evidence for the existence of an acoustical surface wave above porous boundaries is reviewed. Recent measurements including pulse experiments will also be described.

A few years ago the acoustic impedance of a grass-covered surface was measured in the frequency range 30 to 300 Hz. In PART II of this paper further measurements on the same site are discussed. These measurements include core samples, a shallow refractive survey to determine the seismic velocities, and measurements of the acoustic-to-seismic coupling coefficient.

PART I

INTRODUCTION

In atmospheric acoustics, the subject of surface waves above porous grounds has been an area of discussion for many years. The existence of an acoustic surface wave is now well established theoretically. The mathematical solution for spherical wave propagation above an impedance boundary includes the possibility of a contribution that possesses all the standard properties for a surface wave. These include cylindrical spreading in the horizontal direction, exponential decay in amplitude with height above the ground, and a reduced phase speed.

However, above natural porous ground surfaces, the existence of an acoustic surface wave has eluded direct experimental confirmation. Pulse experiments have failed to show a separate arrival from the direct pulse as expected from the reduced phase speed. Further, indirect evidence for its existence has appeared contradictory.

The experimental evidence for surface waves has been mostly restricted to careful indoor measurements, using sources of continuous sound and model surfaces composed of a thin layer of porous material or comblike structures. The reduced phase speed and cylindrical spreading of the surface wave are expected to produce a total sound pressure level in excess of that which would be measured over an acoustically hard boundary.

In this paper the experimental evidence for the existence of an acoustical surface wave above porous boundaries is reviewed. In addition, some recent measurements including pulse experiments will also be discussed.

FIGURE 1

At this point it is useful to distinguish between body waves and boundary waves. Acoustic waves propagating through the body of the fluid are referred to as body waves. The effect of boundaries upon these waves is secondary in that the existence of the waves is in no way tied to the presence of the boundaries. The role of boundaries is strictly extrinsic. On the other hand, boundary waves depend upon the existence of boundaries to support them and the role of the boundaries here is intrinsic.

In atmospheric acoustics, the field from a point source above a porous ground is commonly described in terms of direct, reflected, ground, and surface waves. Obviously ground and surface waves are closely related but their fundamental origins differ, as does their behavior during propagation. Ground waves exist because curved wave fronts strike different parts of the ground at different angles of incidence and because the reflection coefficient of finite-impedance ground is also a function of angle of incidence. Ground waves exist unless the ground is infinitely hard or infinitely soft or unless the incident wave fronts are plane, that is, the source can be considered infinitely far away. Ground waves can exist in the absence of surface waves.

Surface waves exist when the ground surface is sufficiently porous, relative to its acoustical resistance, that it can influence the airborne particle velocity near the surface and reduce the phase velocity of sound waves in air at the surface. In its simplest terms, the condition for its existence is when the imaginary component of the surface impedance is a spring-like reactance and is greater than the resistive component. This traps some of the sound energy in the air, regardless of the shape of the incident sound field, to remain near the surface as it propagates from the source to the receiver. Surface waves can exist in the absence of ground waves. The existence of a surface wave in the absence of wavefront curvature has been shown theoretically by McAninch and Myers (AIAA 1988). They demonstrate the presence of a surface wave in the solution for plane waves at grazing incidence to a finite impedance boundary. Further, Raspet and Baird (JASA 1989) have demonstrated that the surface wave can exist independent of the acoustic body wave in the half-space above the surface by examining the limit as the upper half-space becomes incompressible.

The equation on the top part of this figure represents a particular representation for the total field above an impedance plane. The field is broken up into a direct wave, a perfect reflected wave, a diffracted wave that accounts for the phase change on reflection and the effects of the spherical wave fronts, and a surface wave. The surface wave exists if $\mathrm{Im}(Z) > \mathrm{Re}(Z)$ and is zero otherwise. The surface wave is characterized by cylindrical spreading in the horizontal plane, exponential decay with increasing height above the ground, and a reduced phased speed $v < c$.

Theory which predicts the acoustical characteristics of rigid porous materials in terms of their microstructure indicates that the resistive and reactive components of the surface impedance are equal in the case of a homogeneous porous ground (Attenborough, JSV 1985). Therefore, no surface wave can exist above such grounds. On the other hand, if the microstructural properties of the ground vary with depth (such as a varying porosity), the reactive component of the impedance exceeds the resistive component and the surface wave can exist.

A specific example of a surface whose reactive component of impedance exceeds the resistive component is a thin porous layer above an acoustically hard backing. We note that in the case of a ground where the porosity varies with depth at a rate α, the impedance is equivalent to the impedance of a porous layer with an effective thickness equal to $2/\alpha$ (Donato, JASA 1977).

FIGURE 2

The consequence and origin of the reduced phase speed of the surface wave are illustrated in this figure. Far from the ground, there is horizontal particle motion associated with the propagating body wave, as shown in A. Due to the alternating compression and rarefaction cycles, the air molecules at the ground are entrained in vertical particle motion as shown in C. Just above the surface of the ground in the fluid, the resulting particle motion is therefore elliptical, as shown in B.

The elliptical particle motion results in a reduced phase speed and the resulting lag causes the wavefronts to be "bent" towards the ground, giving rise to enhanced sound energy close to the surface. The increased sound energy associated with the surface wave close to the ground is at the expense of less sound energy at heights above the surface wave thickness. This will be illustrated in some of the following figures.

FIGURE 3

This figure shows experimental evidence measured outdoors over natural ground surfaces. The points in (a) are measurements obtained by Rasmussen above grass covered ground. The sound pressure levels in this figure, and all of the following figures, are plotted relative to free field. Hence, these results suggest sound pressure levels in excess of the +6 dB expected at lower frequencies. The solid curve is the best prediction that can be achieved by assuming the ground to be a semi-infinite half plane. Rasmussen calculated the dashed curve by assuming a porous layer 0.01 m thick. Equivalently, the same result can be obtained by assuming a ground with its porosity varying with dept at a rate given by $\alpha = 2/0.01 = 200\ m^{-1}$. This is a more likely physical model for natural ground surfaces (Donato, JASA 1977).

We note that the behavior of Rasmussen's measurements is consistent with the behavior of the classic measurements of Parkin and Scholes (JSV 1965) of the propagation of jet engine noise above grass covered airport ground.

In (b), the points were measured above a well defined layer (8 cm) of snow above frozen ground. The dashed curve was calculated by assuming a layer of snow infinitely thick. The solid curve accounts for the layer. Although the measurements show the enhanced dip that is predicted around 300 Hz (Chien and Soroka, JSV 1975), the behavior of the measurements at the lower frequencies indicate that the surface wave is absent. These results have contributed to the controversy concerning the existence of surface waves above natural ground surfaces. It has been suggested (Attenborough, JSV 1988) that the situation is complicated by the existence of seismic quarter-wavelength resonances in the low frequency range as a result of the elasticity of the porous surface layer.

FIGURE 4

The short dashed curve on this slide is the sound pressure levels predicted for propagation at grazing incidence above an infinitely thick surface of porous felt. The propagation distance is 2 m. There is no surface wave and this curve represents the ground wave. The open squares are measurements obtained above a thick layer of felt.

The upper two curves are calculated from different versions of the same theory in the case of a layer of felt of thickness 0.003 m. In this case the surface wave Φ_S exists. The difference between the two curves is attributed to numerical precision and is not significant for the discussion here.

The solid points are measurements made by Thomasson above a layer of felt. The open circles are our own measurements and confirm the results of Thomasson. Both theory and experiment clearly indicate sound pressure levels in excess of the +6 dB expected from inverse square law above a perfectly rigid ground.

FIGURE 5

The open points are measurements made as a function of height above the same layer of felt and shown for two frequencies. The solid points were obtained by Thomasson for the same two frequencies. The solid and broken curves are the predictions calculated from two versions of the same theory. The broken curves are the predictions in the case of an infinitely thick layer.

The dotted lines drawn at +6 dB show the levels expected in the case of a perfectly rigid ground. Both theory and measurements show the existence of the enhanced sound levels at heights below 10 cm resulting from the existence of the surface wave. In addition, the slightly reduced levels above about 10 cm, especially at 2 kHz, is observed.

FIGURE 6

In this figure, the porous layer is replaced by a comblike surface consisting of overhead lighting panels (Donato, JASA 1978). The panels are molded plastic: there is a square array of solid ribs at 1.13 cm spacing; the sheet is 2.26 cm thick, open on top and bottom surfaces. The sheet is laid on a hard floor.

Results of measurements are shown for two frequencies and two distances of propagation. The solid points clearly show significantly enhanced sound levels close to the surface, especially at 800 Hz, and the expected reduced level at higher heights.

The open points are the results above a rigid surface and the solid lines are drawn at +6 dB.

FIGURE 7

These results are similar to the ones on the previous slide but the first four meters of the propagation path are acoustically rigid while the remainder consist of the comblike surface.

The solid points to the left are measurements made above the rigid surface. The open points on the right were measured 5 m from the source, hence after 1 m of propagation above the ceiling panels.

The behavior of the results at 5 m suggest that a surface wave has developed over the

1 m of panel. We note that the panels are located about 12 wavelengths from the source. Therefore the surface wavelike behavior is exhibited when the curvature of the wavelength is significantly reduced. This is consistent with the theory of McAninch and Myers.

FIGURE 8

The solid points on the top part of this figure are the results measured at grazing incidence above the comblike surface as a function of frequency for a distance of 1 m. The behavior of these results is identical to those measured above the layer of felt.

The solid curve on the bottom part of the figure shows the predicted surface wave velocity, v (Brekhovskikh, Sov. Phys. Acoust. 1959). The straight line at about 340 m/s indicates the speed of the body wave in air. Beyond about 1.5 kHz there is a sufficient difference between the surface wave velocity v and the body wave velocity c, that it should be possible to observe the surface as a separate arrival using a short pulse of sound propagating over a distance of a few meters.

FIGURE 9

The traces shown here are of a 2.1 kHz tone burst measured after propagation above the comblike surface at various distances up to 1.5 m. The arrow immediately below the last three traces indicates the arrival of the surface wave relative to the body wave predicted from the solid curve on the previous slide.

The observed behavior of the measured pulses as a function of distance is not inconsistent with expectations. In the absence of a surface wave all the traces would have the appearance of the top trace.

FIGURE 10

This figure shows the traces at different receiver heights for three distances of propagation (the source is on the ground). At a distance of 0.1 m, the surface wave has not yet had time to develop and the trace does not change with height.

At the other two distances, the exponential decay of the second arrival as a function of height is clearly illustrated and is indicative of a surface wave.

PART II

INTRODUCTION

A few years ago the acoustic impedance of a grass-covered surface was measured (Daigle and Stinson, JASA 1987) in the frequency range 30 to 300 Hz by measuring the pressure, phase and phase-gradient in the sound field along a vertical line directly below a loudspeaker suspended some 7 m above the surface. Recent core samples showed that this ground consisted of a layer of silt of uniform texture and almost constant thickness (1.6 +/- 0.3 m) over bedrock -- a ground structure of ideal simplicity for acoustical study. Seismic velocity measurements were consistent with this simple structure, and indicated a layer thickness (1.9 +/- 0.3 m) reasonably in agreement with the core sample.

The calculated quarter-wavelength-layer-thickness frequency is then about 45 Hz. Direct measurement of the acoustic-to-seismic coupling coefficient at normal incidence shows maxima in the admittance of the surface at about 50 and 135 Hz. (Several other maxima exist at apparently unrelated frequencies.) At oblique angles of incidence the admittance spectrum is of similar shape but shifts upwards in frequency by about 10%.

A number of minima in the admittance spectrum are also present and should correspond with maxima in the acoustic reflection coefficient; however, the correspondence was found to be poor. Probable explanations of the discrepancies could be that the ground exhibits in reality a more complex structure than our current understanding allows or that different measurements were over slightly different areas of the ground and detected different thicknesses of the supposedly constant thickness silt layer.

FIGURE 11

This figure illustrates the original measurements. A pure tone is radiated spherically from a loudspeaker suspended resiliently from a support. Wavefronts are reflected at the ground surface and interfere with the incoming waves to produce an interference field. Two closely spaced microphones were moved together along a track that was perpendicular to the surface and directly below the source. By comparing the signals from the two microphones with each other and with the electrical signal to the source, one can determine the amplitude, phase and phase gradient of the field along the line of measurement. The locations where one of these three parameters becomes inaccurate are usually those where the other two parameters can be measured with enhanced precision. In this way the magnitude and phase of the reflection coefficient can be obtained reasonably accurately down to 30 Hz.

FIGURE 12

This figure shows the results. Although the individual points show some scatter there are definite trends and several peaks, or resonances are clearly evident. For example there is some confidence in the peaks at around 95, 130 and 200 Hz. These seismic resonances are consistent with the theoretical work and measurements of Sabatier, Bass and others at the University of Mississippi.

In 1989 a seismic survey team drilled one or two core samples on our exact site. It was discovered that our site was almost ideal from an acoustical point of view. Apart from the top few centimeters of grass and its roots, the ground was a layer of silt of uniform consistency and almost constant thickness (1.6 +/- 0.3 m) lying directly over bedrock.

FIGURE 13

Time-of-flight measurements along the surface are shown in this figure. These were made by hitting a heavy metal disk lying on the ground with a hammer, and receiving the signal with a geophone. The sound speed in the silt layer is calculated to be 330 m/s (almost the same as the speed in air) and in the rock about 2000 m/s. From the break-point on this curve the thickness of the layer is calculated as 1.9 +/- 0.3 m. The $v = 330$ m/s part of this plot does not pass through the origin but intersects the ordinate at about $t = 3.8$ ms. This time delay is related to the slow sound speed through the top few centimeters of soil and grass-roots, but we were not able to measure the break-point due to the soil-silt interface. The calculated quarter-wavelength-layer-thickness resonance for the silt layer is about 45 Hz.

FIGURE 14

The acoustic-to-seismic transfer function was measured using a Mark Products L-21A geophone pushed into the ground surface and a collocated microphone 10 cm above the surface. The two signals were analyzed and compared using a Bruel and Kjaer Model 2032 Dual Channel Signal Analyzer. The acoustic-to-seismic transfer function was found for various angles of incidence ranging from normal to about 87^{o}. Those for normal incidence and for 84^{o} are shown in Figure 14. Measurements at oblique incidence show a) larger surface admittance, b) smoother curves, and c) an upward shift in frequency by about 10%, compared with the admittance spectrum for normal incidence.

Quarter-wavelength resonances in the silt layer should lead to maxima in the acoustic-to-seismic admittance spectrum at roughly 45, 135 and 225 Hz, and minima at 90 and 180 Hz. The only apparent agreement seems to be maxima at about 50 and 135 Hz and a minimum at about 85 Hz. Although the results could suggest a peak around 225 Hz and a dip at a frequency slightly greater than 180, the measurements are inconclusive. The peaks at about 70, 105 and 180 Hz appear to be completely unrelated to the silt layer. Some of this structure could be due to the thin layer of topsoil and grass roots.

Maxima in the acoustic reflection coefficient of the surface, Figure 12, should be related to the minima of the surface admittance spectrum, Figure 14. The match between these two spectra is far from satisfactory. However, the peaks of the reflection coefficient at about 95 and 195 Hz are not inconsistent with the dips in the admittance spectrum at roughly the same frequencies and are predictable, within experimental, from the thickness of the layer found from the core sample or the refractive survey. The peak at about 135 Hz in the reflection coefficient is unrelated, but the admittance spectrum does suggest a dip at about this frequency.

Clearly, although our current understanding allows us to explain many aspects of these measurements, there are other features of this rather simple ground structure that require additional elucidation. Certainly more work is required before we can accurately predict the acoustical behavior of more realistic and complex ground structures.

ACKNOWLEDGEMENT

The refractive survey and measurements of the acoustic-to-seismic transfer function were carried out by C. Verhaegen (Katholieke Universiteit Leuven, Belgium) during a one month stay as a guest scientist in our laboratory at the National Research Council. We would also like to acknowledge the technical assistance provided by R. St-Denis.

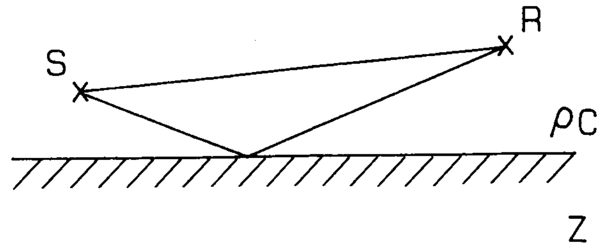

Total field

① $$\Phi = \Phi_D + \Phi_R + \Phi_d + \Phi_s$$

$$\Phi_s = \begin{cases} \text{Surface wave if } \mathrm{Im}(Z) > \mathrm{Re}(Z) \\ 0 \quad \text{otherwise} \end{cases}$$

$$\Phi_s \propto \frac{1}{\sqrt{r}} e^{-\alpha h + i\beta r}$$

Surface wave velocity

Fig. 1

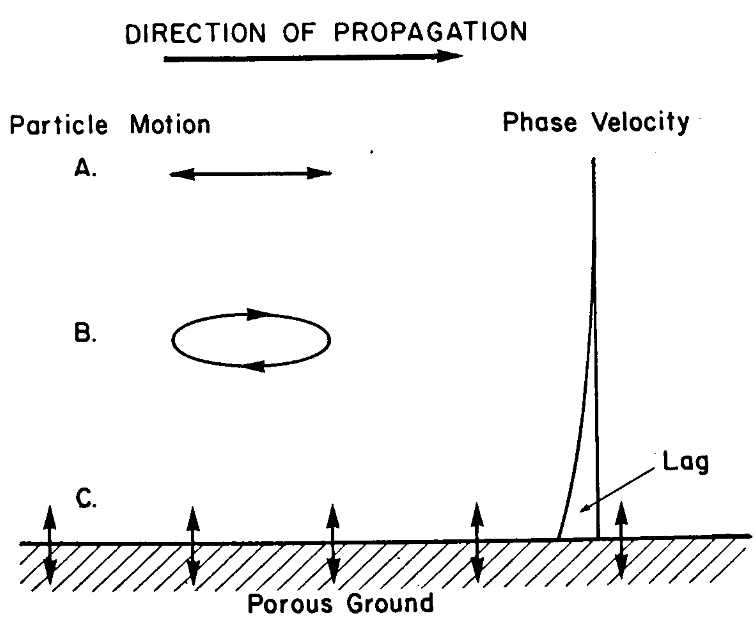

ORIGIN OF THE SURFACE WAVE

Fig. 2

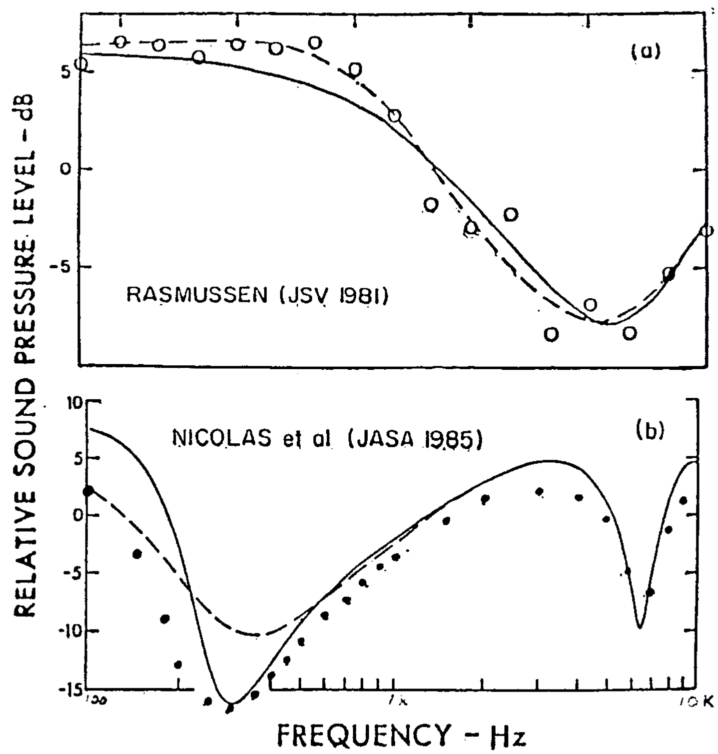

RELATIVE SOUND PRESSURE LEVEL - dB
(a)
RASMUSSEN (JSV 1981)
NICOLAS et al (JASA 1985)
(b)
FREQUENCY - Hz

Fig. 3

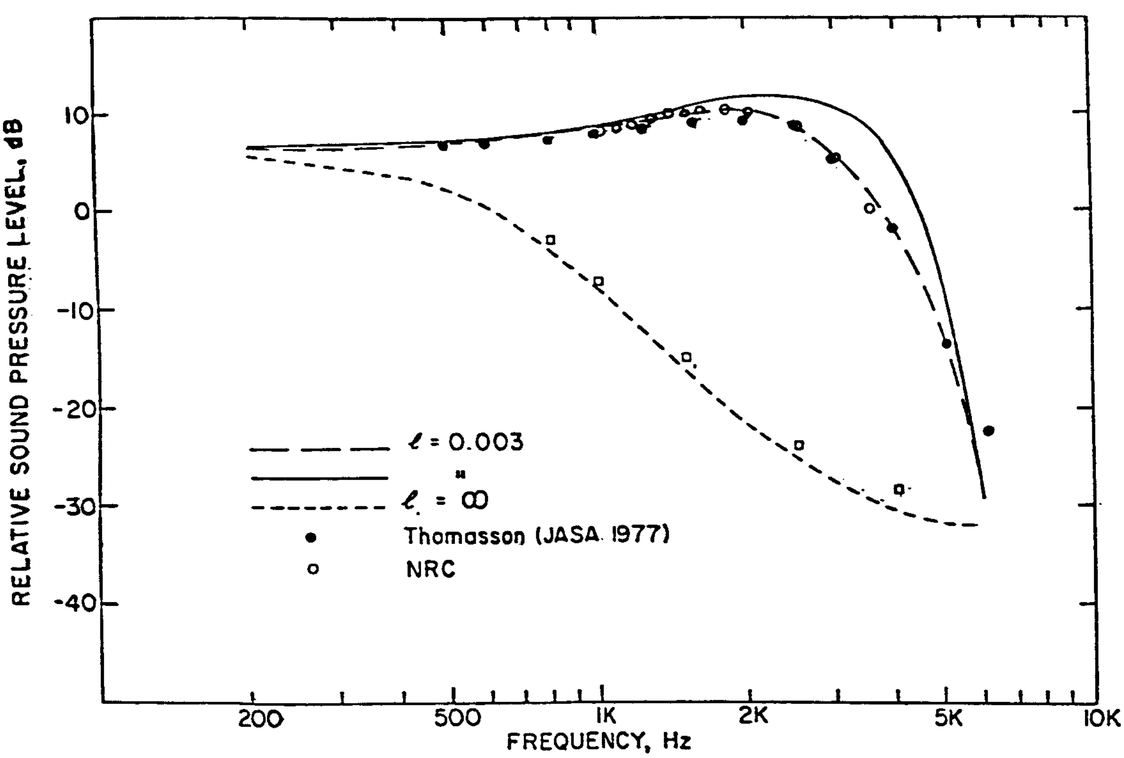

RELATIVE SOUND PRESSURE LEVEL, dB
ℓ = 0.003
"
ℓ = ∞
Thomasson (JASA 1977)
NRC
200
500
1K
2K
5K
10K
FREQUENCY, Hz

Fig. 4

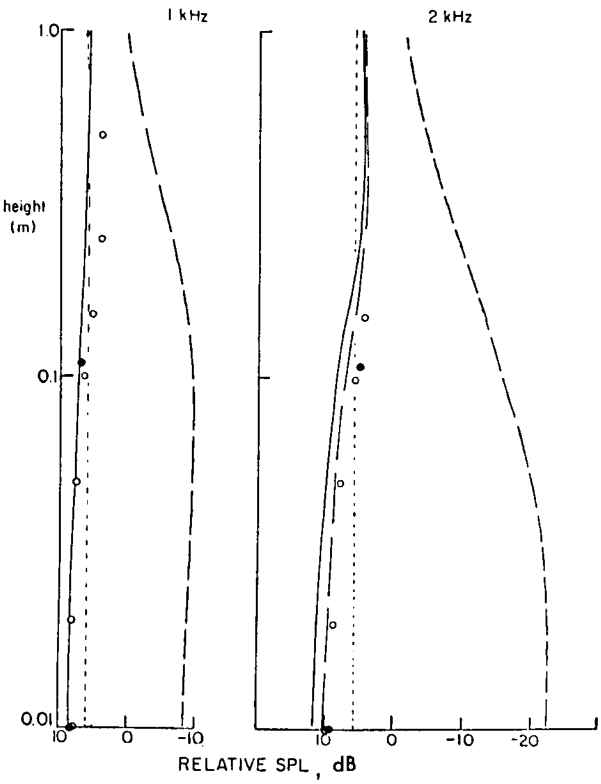

1 kHz
2 kHz
height (m)
1.0
0.1
0.01
10
0
-10
-20
RELATIVE SPL, dB

Fig. 5

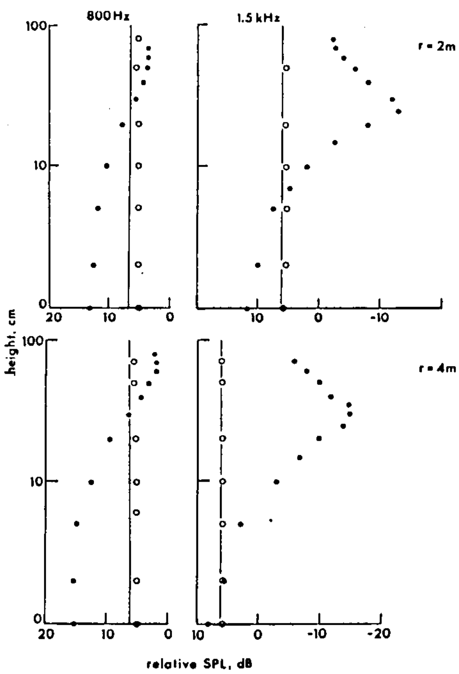

800 Hz
1.5 kHz
r = 2m
r = 4m
height, cm
100
10
0
20
10
0
-10
-20
relative SPL, dB

Fig. 6

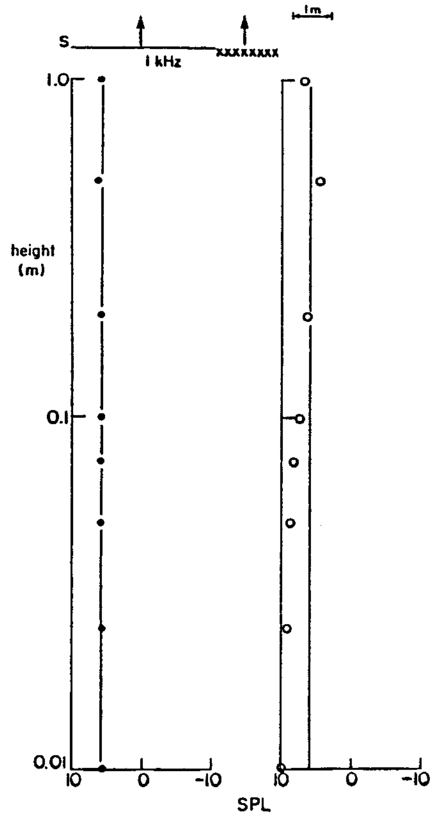

Fig. 7

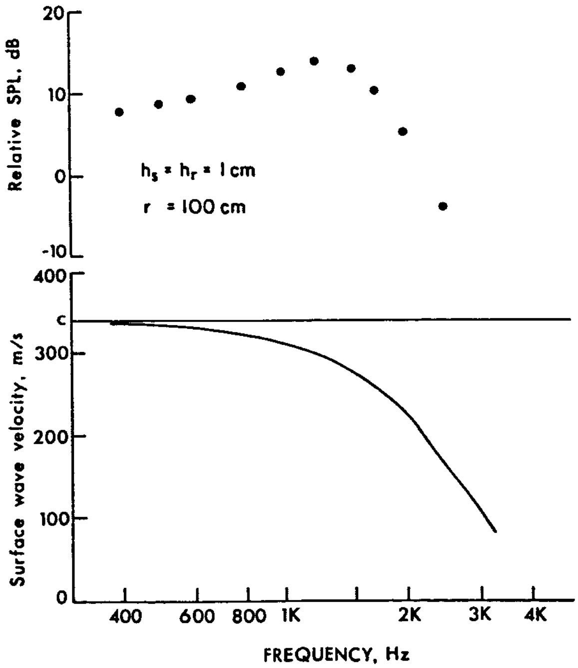

Fig. 8

ORIGINAL PAGE IS
OF POOR QUALITY

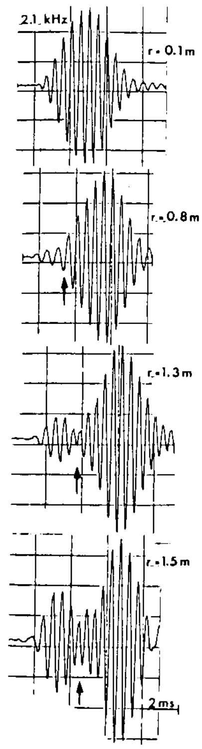
2.1 kHz
r = 0.1m
r = 0.8m
r = 1.3m
r = 1.5m
2ms

Fig. 9

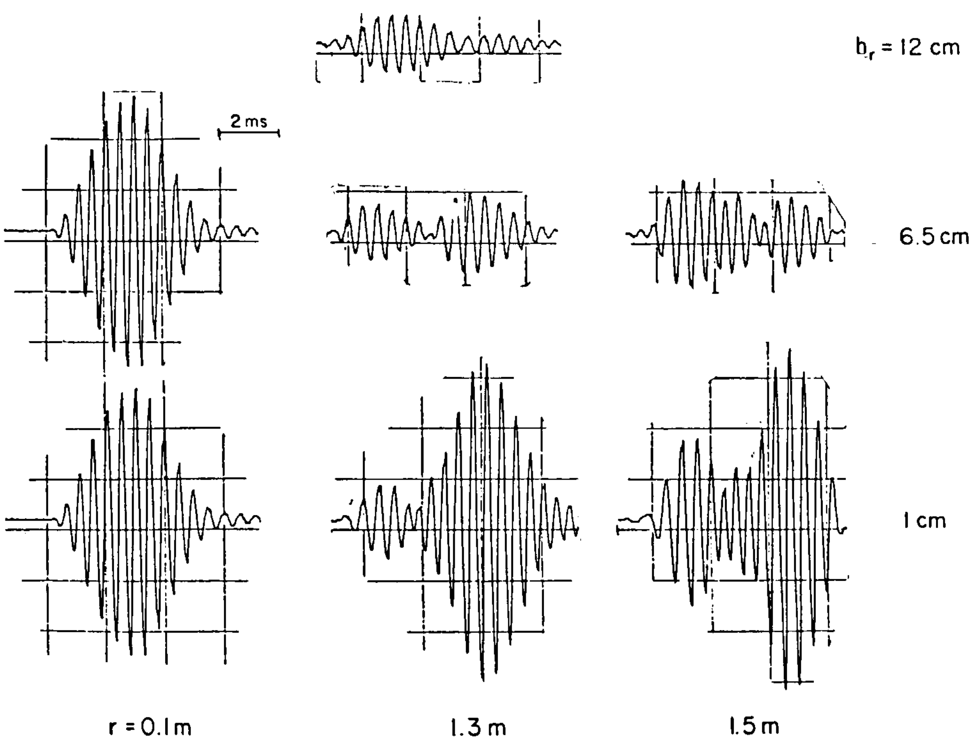
b_r = 12 cm
2 ms
6.5 cm
1 cm
r = 0.1m
1.3 m
1.5 m

Fig. 10

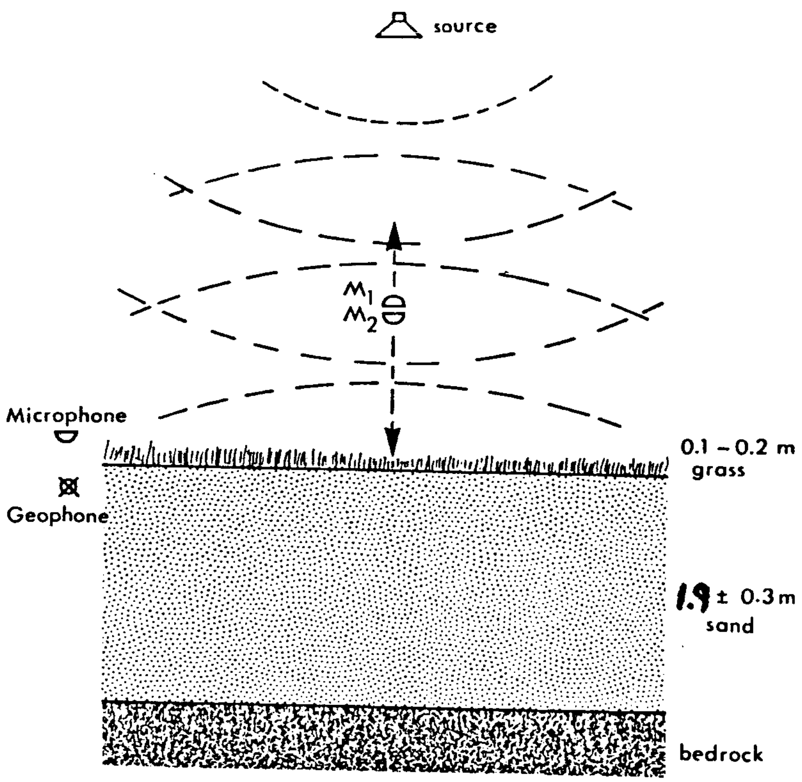

Fig. 11

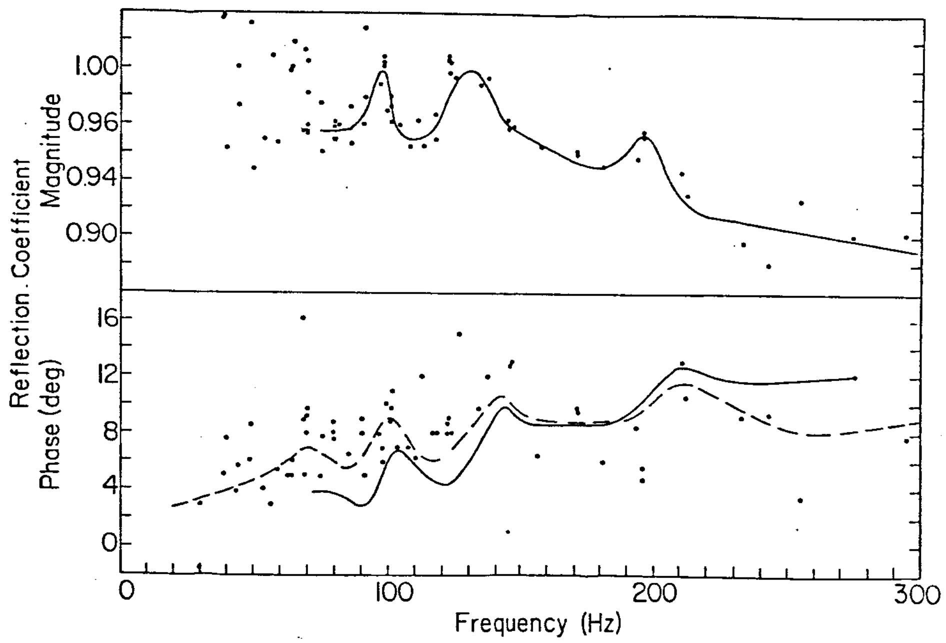

DAIGLE & STINSON(JASA 1987)

Fig. 12

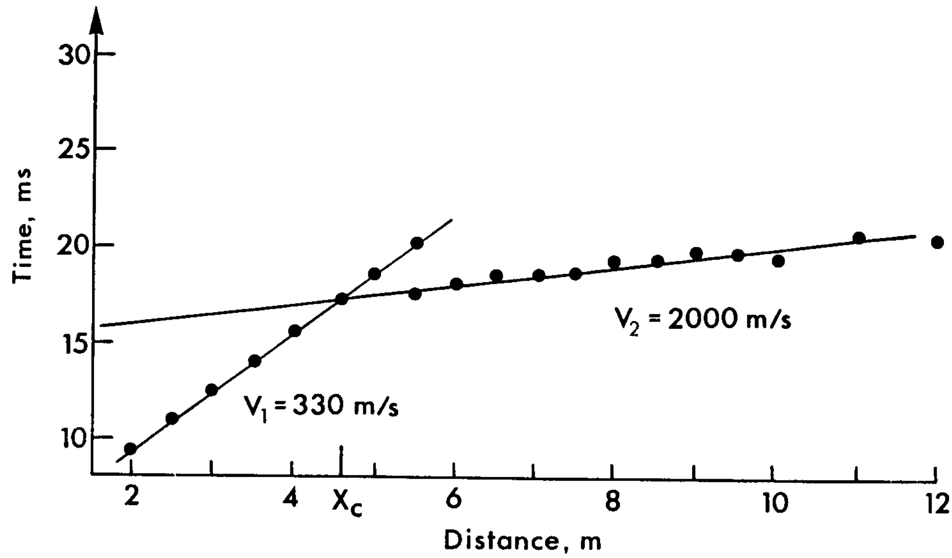
Time, ms
30
25
20
15
10
2
4
X_c
6
8
10
12
Distance, m
V_1 = 330 m/s
V_2 = 2000 m/s

Fig. 13

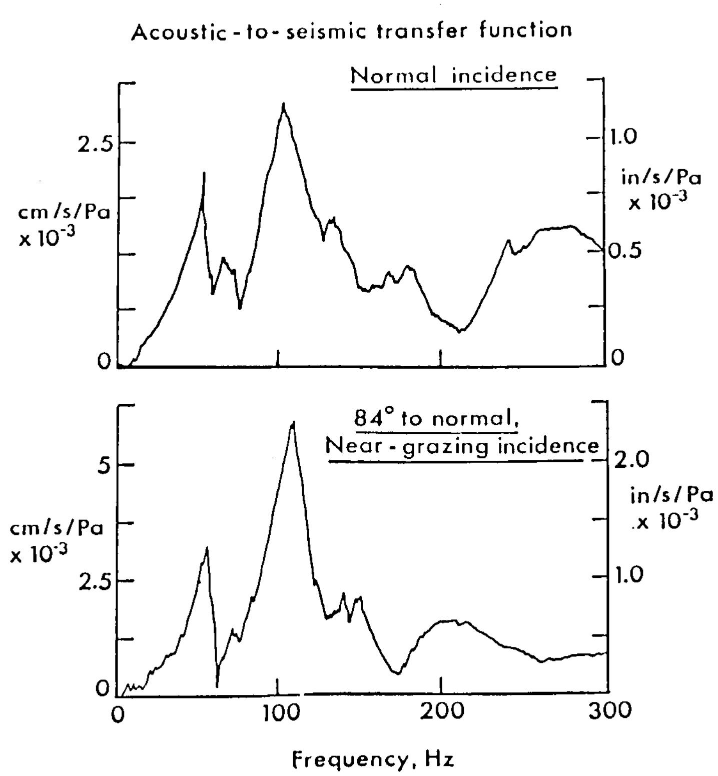
Acoustic-to-seismic transfer function
Normal incidence
cm/s/Pa x 10^{-3}
2.5
0
1.0
in/s/Pa x 10^{-3}
0.5
0
84° to normal,
Near-grazing incidence
cm/s/Pa x 10^{-3}
5
2.5
0
2.0
in/s/Pa x 10^{-3}
1.0
0
100
200
300
Frequency, Hz

Fig. 14